INTERNATIONAL JOURNAL OF INTEGRATED ENGINEERING
ISSN: 2229-838X e-ISSN: 2600-7916

IJIE

Vol. 16 No. 6 (2024) 130-144
https://publisher.uthm.edu.my/ojs/index.php/ijie

Energy Absorption Performance of Hybrid Bamboo Fibre/Aluminium Mesh Reinforced Polymer Composites Subjected to Axial Crushing Loads

Nik Ainun Nik Ismail[1,2], Mohd Nazrul Roslan[1,5]*, Al Emran Ismail[3] , Mohd Khairun Anwar Uyup[4]

[1] *Faculty of Engineering Technology, Universiti Tun Hussein Onn Malaysia, Pagoh Campus, 84600 Pagoh, Johor, MALAYSIA*
[2] *Institut Kemahiran Tinggi Belia Negara, Pagoh, KM 21, Jalan Panchor, 84600 Muar, Johor, MALAYSIA*
[3] *Faculty of Mechanical and Manufacturing Engineering, Universiti Tun Hussein Onn Malaysia, 86400 Parit Raja, Batu Pahat, Johor, MALAYSIA*
[4] *Forest Research Institute Malaysia, 52109 Kepong, Selangor Darul Ehsan, MALAYSIA*
[5] *Bambusoideae Technology Sdn Bhd, No 2.D.1.047, Blok D, Universiti Tun Hussein Onn Malaysia, Pagoh Campus, 84600 Pagoh, Johor, MALAYSIA*

*Corresponding Author: nazrul@uthm.edu.my
DOI: https://doi.org/10.30880/ijie.2024.16.06.013

Article Info

Received: 26 August 2024
Accepted: 14 October 2024
Available online: 4 November 2024

Keywords

Aluminium mesh sheet; axial crushing loads; bamboo fibre; bamboo nonwoven mat; energy absorption; hybrid composite

Abstract

This study examines the energy absorption capabilities of polymer composites reinforced using a hybrid combination of bamboo fibre and aluminium mesh. The fabrication of the composites involves the utilisation of epoxy resin as a matrix material, which is reinforced with bamboo fibre and an aluminium expanded mesh sheet. This is achieved using the vacuum infusion method, where different stacking sequences and mesh sizes are employed. Two distinct types of tests were conducted in this study: a quasi-static axial crushing test and a dynamic impact test. A comprehensive examination has been conducted to investigate the failure mechanism of the specimens during both testing phases. The energy absorption performance of the specimens has subsequently been evaluated. The findings indicate that specimen A3L exhibited the maximum energy absorption and specific energy absorption compared to all other specimens in both tests. Conversely, specimen A1S demonstrated the lowest energy absorption performance during the test. When comparing the lowest and highest values, this study found that the Energy Absorption (EA) and Specific Eenergy Absorption (SEA) values increased by up to 230% and 125% during the quasi-static test and by 273% and 148% during the dynamic test. An analysis of variance (ANOVA) was conducted on the collected data from both tests in order to determine the elements that significantly impact the energy absorption performance of these composites.

1. Introduction

The rapid advancement of vehicle production necessitates an emphasis on ensuring that the vehicles produced are safer for users. There are numerous factors that can be improved to make the vehicle structure safer. The

This is an open access article under the CC BY-NC-SA 4.0 license.

primary design consideration that necessitates attention pertains to the vehicle's structural design and material composition [1], [2], specifically its enhanced energy absorption capacity. This refers to the structure's ability to absorb and dissipate energy effectively during impact events. From a technical standpoint, the phenomenon of energy absorption is intricately linked to crashworthiness. The primary objective in designing crash-worthy systems with minimal weight is optimising energy absorption while minimising mass. The growing use of fibre-reinforced polymer (FRP) composites in vehicle structure manufacturing has led to the extensive replacement of metals.

The FRP composite possesses a remarkable strength-to-weight ratio and stiffness, which can effectively decrease the bulk of the vehicle [3]. The utilisation of FRP composite energy absorbers has garnered widespread acceptance within the academic community due to their potential to enhance crashworthiness while maintaining weight efficiency through meticulous design considerations. Hence, the pursuit of lightweight design utilising FRP materials has garnered significant attention, primarily driven by the imperative to curtail fuel consumption and mitigate environmental pollution, particularly within the realm of the transportation sector [4], [5]. Consequently, it can be inferred that a well-crafted composite design will yield a greater degree of efficacy in terms of energy absorption when compared to metallic materials [6], [7].

The utilisation of Fibre Reinforced Polymers (FRPs), including carbon fibre reinforced polymer composites and glass fibre reinforced polymer composites, has demonstrated notable advantages, particularly in enhancing material strength and reducing overall weight. However, it is crucial to acknowledge that their application also presents certain environmental challenges. Environmental issues have emerged as significant global challenges, garnering the interest of scholars, scientists, engineers, and environmental advocates who are actively engaged in the exploration and creation of alternative materials that are conducive to ecological preservation [8]. The utilisation of natural fibres has garnered significant attention as a means to decrease dependence on synthetic fibres for high-end composite applications, primarily due to the ecological concerns associated with the life cycle of synthetic fibres. In recent years, a multitude of studies have been undertaken to investigate the application of natural fibre-reinforced composites in the realm of energy absorption [9].

Bamboo has emerged as a prominent natural fibre source that has garnered significant attention among researchers in recent times. The mechanical properties of bamboo fibres exhibit notable characteristics, including elevated levels of strength, a reduced specific weight ratio, enhanced tensile strength, and a superior modulus of elasticity when compared to select natural fibres. Bamboo, recognised as a natural glass fibre possessing comparable tensile strength to that of bamboo fibre bundles, exhibits a tensile strength equivalent to that of jute fibre [10], [11]. Concurrently, additional scholars have posited that the robustness of bamboo renders it a compelling substitute for steel in scenarios involving tensile loading [12]. Nevertheless, it is imperative to acknowledge that natural fibres are significantly prone to thermal and hygroscopic stresses, while also demonstrating restricted mechanical properties due to variations in fibre dimensions and uneven interfacial strength [13]. Additionally, [14] asserted that an ideal material for energy-absorbing tube properties could not be achieved by any singular natural fiber material. Hybridisation is therefore a viable method for enhancing this characteristic, particularly in the case of plant fibres.

The hybrid composite technique involves the combining of several fibres with distinct elements inside a unified matrix. Hybrid composites are more affordable than regular composites and have special qualities that can be utilised to meet a variety of design requirements [15]. An abundance of studies have been documented about the hybridisation of composites with the aim of enhancing their mechanical, physical, and thermal properties [16]–[22]. The observed enhancement is attributed to the heightened bonding between fibres or between fibres and the matrix during the process of hybridisation. Hybrid composites encompass a diverse range of compositions, which are contingent upon the specific combination of fibres employed. One example pertains to a hybrid composite material that integrates both metallic and fibrous components.

Aluminium is one of the preferred metals for utilisation in the composite hybridisation process owing to its comparatively lower cost, reduced weight, and enhanced strength in comparison to alternative metals. The utilisation of aluminium hybridised with synthetic fibres has been documented in numerous studies on composites, with various researchers asserting that this approach has the potential to enhance the mechanical properties of the resulting hybrid composites [23], [24]. A study conducted by [25] investigated the tensile characteristics of hybrid fibre metal laminate (FML) composites, including a small amount of aluminium alloy and aramid fabric as the reinforcement. The results of the tensile testing indicated that FML exhibits greater ductility than its individual components, as seen by a 230% increase in strain at failure. Similarly, the aramid fabric composite laminate demonstrated a 400% increase compared to the aluminium sheet. A separate investigation conducted by [26] centred on analysing the influence of hybrid FML composed of aluminium, carbon, and glass fibres as reinforcing materials. The findings of the study indicate that the hybrid of glass, carbon and aluminium composites had a greater capacity to absorb impact loading compared to the hybrid of glass and aluminium composites. The observed enhancement in impact resistance can be attributed to the use of carbon fibres with high stiffness.

Int. Journal of Integrated Engineering Vol. 16 No. 6 (2024) p. 130-144

Despite the favourable mechanical properties demonstrated by hybrid FML composites, the composite remains susceptible to certain drawbacks. As an illustration, the interface toughness between aluminium and its fibre layers is quite modest. As a result, research has been conducted to determine how to enhance the interface bonding of this reinforcement. An approach that has been proposed is the substitution of aluminium sheet with aluminium wire mesh [27], [28]. In comparison to the glass fiber-reinforced polymer composite, the tensile strain was enhanced by 54% and the flexural strain was increased by 117.5% with the addition of aluminium wire mesh layers as found in [27]. The ductile deformation of the aluminium layers was facilitated by the inclusion of aluminium mesh in the initial and final layers, which exhibited the greatest shear and normal stresses, consequently augmenting the failure strain. In addition, the energy absorption capacity exhibited an enhancement in tensile and flexural experiments when compared to polymer composites reinforced with glass fibres. As such, the hybridisation of aluminium wire mesh with bamboo fibres in the form of FML structures is the subject of this investigation, given the paucity of prior research in this area.

Numerous crucial insights and benefits pertaining to the reinforcement of the composite with bamboo fibres and aluminium have been discussed. Due to the distinct properties of both substances, the hybridisation investigation can be carried out. A dearth exists in durable hybrid polymer composites reinforced with aluminium and bamboo fibres. These composites are indispensable for critical applications as a substitute for commercially available synthetic composite materials. This research aims to create a new type of composite material, called a hybrid bamboo fiber/aluminum reinforced polymer (BFAMRP) composite, in the shape of plates. The purpose of this material is to absorb energy in various applications. The development of this composite will be achieved by axial compression experiments and simulation. With high-strain deformation and aluminium reinforcement, a high energy absorption capacity could be achieved, according to the hypothesis underlying this investigation. On the contrary, by increasing the surface area generated by bamboo fibre reinforcement during impact and collision, the overall weight of the novel BFAMRP composite could be reduced.

2. Materials and Method

2.1 Materials Preparation

This study employed bamboo fibre nonwoven preform and aluminium expanding mesh as reinforcements. The bamboo fibre was obtained from Buluh Semaliang, scientifically known as Schizostachyum Grande, and was supplied by HangterraBamboo Sdn Bhd. This study used two different sizes of expanded aluminium mesh: 3.5 mm x 2.0 mm for the small mesh and 4.0 mm x 3.0 mm for the large mesh. Both of the aluminium meshes were bought from China. The matrix combination consisted of thermoset polymer resin epoxy 1006, which was supplied by Wee Tee Tong Chemicals Pte Ltd, located in Sungei Kadut, Singapore.

For this study, specimens in the form of composite panels have been produced by using a vacuum infusion process (VIP) comprising a length (l) of 60mm and a width (w) of 30mm. In order to prevent a sudden increase in peak force and the possibility of an unstable collapse, a 45° chamfer was created on the top of the specimens, as depicted in Figure 1. Eight types of composite panels were designed and prepared, as shown in Table 1.

2.2 Quasi-Static Axial Crushing Test

The quasi-static axial crushing test is commonly used to determine the energy absorption of composites when they are crushed under axial loads. The test for this study was based on the approach provided by [29]. Victor, Material Testing Equipment, located at the Automotive System Lab, Faculty of Mechanical Engineering Technology, UTHM, was employed for the test.

All eight types of composite were subjected to the quasi-static crushing test and have been set up as shown in Figure 2. A small fixture was utilised to hold the samples during the test to ensure that they remained stable during the crushing test. For all specimens, the testing rate was set at 2mm/s. During crushing, a computer-aided data-collecting system recorded the load-displacement curve to calculate the Energy Absorption (EA) for each sample. The EA can be calculated by using Equation1. Other item that were analyzed for this test were Specific Energy Absorption (SEA), Crush Force Efficiency (CFE), the max force during crushing (Fmax) and average force throughout the test (Favg).

$$EA = \int F \mathrm{dl} \qquad \text{(Equation 1)}$$

Where F and dl are the crushing force and crush distance, respectively.

2.3 Dynamic Impact Test

The Instron Drop Weight Impact machine was used to perform the dynamic impact test. The parameter for this test was selected based on the maximum impact energy obtained from the quasi-static test. The tests were

conducted exclusively at the Composite Centre of UTM Skudai. The machine is a stationary impact device capable of delivering energy ranging from 0.3J to 1800J. The machine was outfitted with a DAS 64K data collecting system that had a maximum sampling rate of 4 MHz.

Figure 3 illustrates the placement of the plate specimen on the flattened metal. The flat impactor, equipped with a load cell capable of measuring force, was securely attached to the machine with a weight placed on top. Subsequently, the flat impactor was employed to pulverise the specimen. The data-collecting program automatically generates energy absorption and impact velocity data rather than load-displacement data. Subsequently, the findings of the dynamic crush test can be compared to the quasi-static crush test results obtained from the quasi-static test to examine different crush loadings related to energy absorption capacity and other crushing performances.

2.4 Analysis of Variance (ANOVA)

The energy absorption performance of the BFAMRP composite was statistically analysed using the general linear model (GLM) of analysis of variance (ANOVA) using MINITAB 19 Software. The analysis was performed using a significance level of 5%.

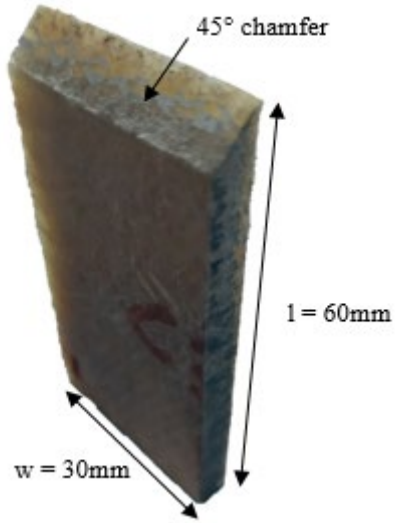

Fig. 1 *Specimen characteristics*

Table 1 *Specimen details*

No	*Specimens code	**Reinforcement domination	**Weight fraction (%)		Total weight	Stacking sequence (structure)	Mesh size
			A	B			
1	A1S	3A2B	53.7	46.3	162.12	Al mesh Bamboo fiber Al mesh Bamboo fiber Al mesh	S
2	A1L		63.3	36.7	198.97		L
3	S2S		54.1	45.9	160.72	Bamboo fiber Al mesh Al mesh Al mesh Bamboo fiber	S
4	S2L		62.6	37.4	201.15		L
5	A3S	2A3B	35.0	65.0	165.48	Bamboo fiber Al mesh Bamboo fiber Al mesh Bamboo fiber	S
6	A3L		43.9	56.1	191.54		L
7	S4S		38.7	61.3	149.74	Al mesh Bamboo fiber Bamboo fiber Bamboo fiber Al mesh	S
8	S4L		45.8	54.2	183.32		L

* First letter indicated stacking structure; A - alternate structure, and S - sandwich structure
*Middle number indicated stacking sequence
*The last letter indicated the size of the mesh: S – small mesh, and L – large mesh
** A – Aluminium expanded mesh, B – Bamboo fibre nonwoven mat

Int. Journal of Integrated Engineering Vol. 16 No. 6 (2024) p. 130-144

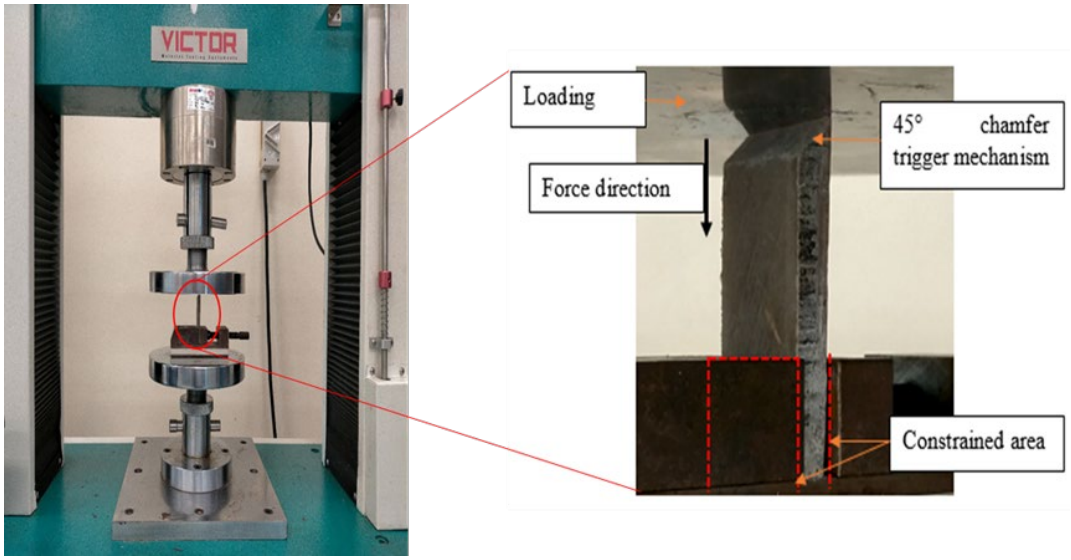

Fig. 2 *Specimen and machine set up for quasi-static axial crushing test*

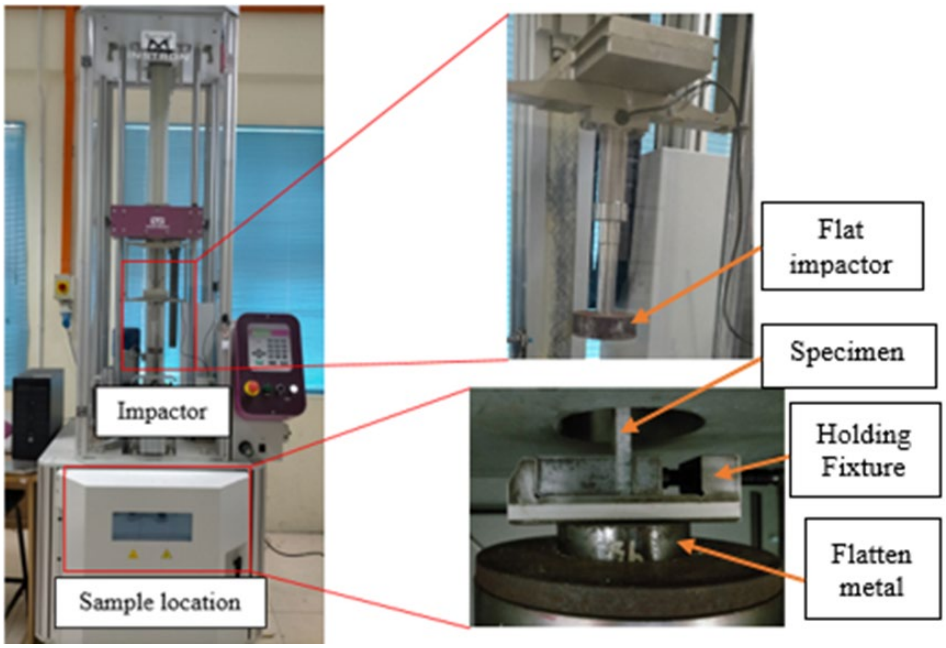

Fig. 3 *Specimen and machine set up for dynamic impact test*

3. Results and Discussion

3.1 Quasi-static Axial Crushing Test

Figure 4 demonstrates that all specimens exhibited a consistent pattern in the load-displacement curve, with the load steadily rising until reaching its peak as a result of progressive failure. According to reports by [30] and [31], there are typically multiple modes of failure for plate hybrid composites. These modes include the progressive failure of the trigger, local and global buckling of the specimens, and specimen rupturing as the final failure mode. When the samples started to buckle and eventually started to break, the load eventually dropped. This research distinguished between two collapsible modes of post-crushing stage behaviour: Mode I and Mode II. Mode I failure was characterised by the concurrent occurrence of local buckling, rupturing, and progressive failure in the specimens. This failure predominantly took place beneath the chamfered region and led to a precipitous decrease in the load curve. This type of failure is found for specimens A1S, A1L, S2S and S4S. In contrast, specimens exhibiting Mode II failure demonstrated a concurrent progressive failure and rupture in the specimen's wall in close proximity to the fixture area. This resulted in an extra displacement prior to complete

failure, which was not observed in specimens exhibiting Mode I failure. Specimens S2L, A3S, A3L and S4L show the Mode II collapsible modes.

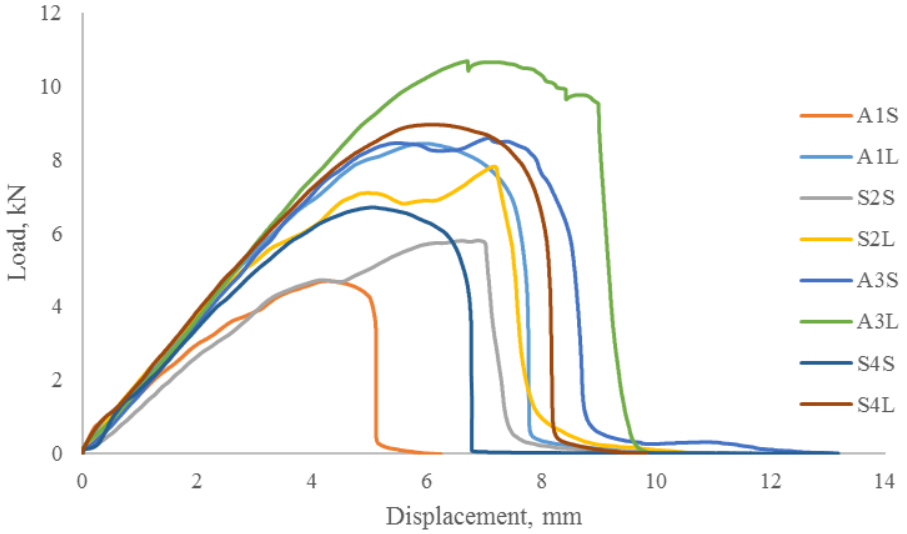

Fig. 4 *Load-displacement curve of all specimens under quasi-static crushing test*

Observations at four sites corresponding to A, B, C and D are shown in Figure 5 and Figure 6 to further validate and examine the particular damage behaviours of specimen A1S (Mode I) and A3L (Mode II) under quasi-static crushing test. Figure 5 shows the specimens were crushed from the top to the chamfer. Starting from point A to point B, the panel was seen to undergo progressive failure and core crushing. The composites suffered fibre compression failure and mild core delamination from point A to point B. After *F*max loading, the sample's load dropped quickly, whereas it normally increased during pre-crushing. As the loading plate was compressed more, the plate specimens started to experience buckling and rupturing, as can be shown in point C onwards. The panel specimen's rupture initiation was indicated by the slightly lower load value between points C and D. The specimen's panel was fully ruptured when it arrived at point D. Cracks around the chamfered area ruptured, causing the specimens to fail under load. The panel buckles completely as tremendous stress builds in the limited area [32].

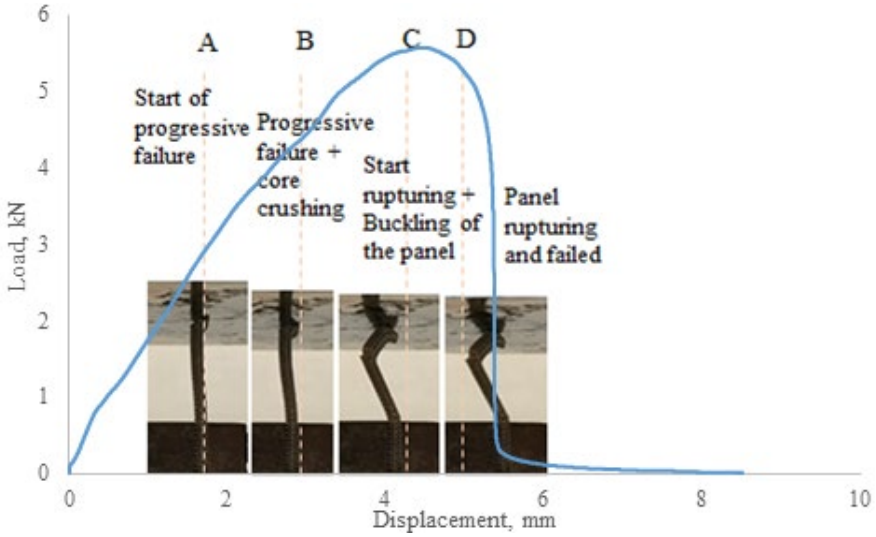

Fig. 5 *Details of Mode I (A1S) crushing mechanism*

Fig. 6 shows a quite nearly identical load-displacement curve in the pre-crushing section to that in Fig. 5. Nevertheless, a notable distinction was observed in the descending trajectory of the section subsequent to compression. After the *F*max value was attained, the load-displacement curve exhibited greater stability and descended gradually over a period of time that was relatively stable. This facilitated a more gradual deterioration of the specimens as opposed to an abrupt failure that would have adverse repercussions for the consumer. Regarding the crushing image, the chamfered portion of specimens experienced a gradual crushing process, wherein the core crushing mechanism significantly contributed to the resistance against the crushing

Int. Journal of Integrated Engineering Vol. 16 No. 6 (2024) p. 130-144

effects (point A to point B). In an effort to withstand the applied force, the specimens continued to deform (point B to point C) until a fracture was identified in close proximity to the support, at which juncture the specimens ultimately failed (point D). Comparable failure conditions have been documented for these specimens in the past by [30]–[33].

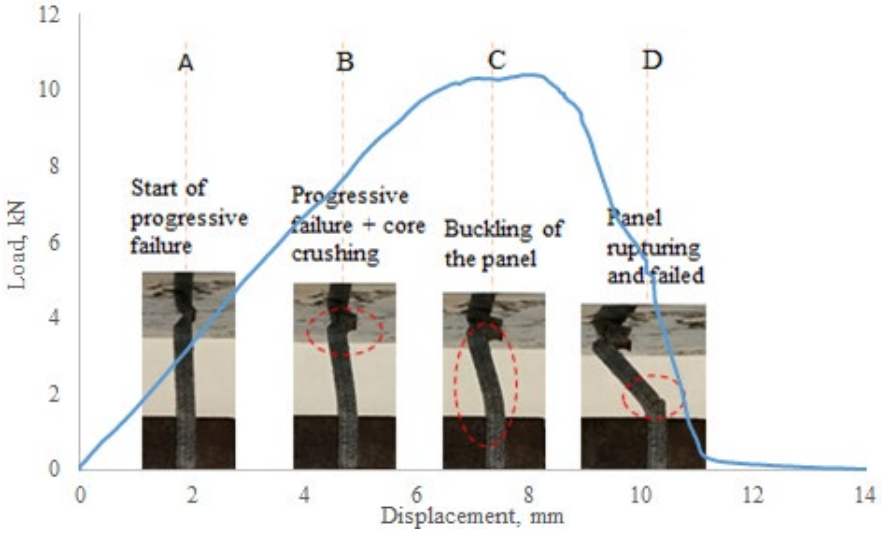

Fig. 6 *Details of Mode II (A3L) crushing mechanism*

Fig. 7 presents the photographic images of the damage morphology obtained from specimen A3L. Specimens after crushing show various types of damage such as fibre breakage, matrix cracking, delamination, aluminium elongation and splaying. The outer layer of laminate was observed to splay outwards. The damage mode observed on the specimen's aluminium mesh sheet suggests that ductile aluminium underwent elongation under the influence of an axial compression load. The placement of aluminium in the specimen's centre, which functioned as a core, retained all components effectively during compression. The brittle fibre layer and plastic aluminium sheet exhibited a potent interactive effect during axial splaying, which prevented the arbitrary deformation of two distinct materials [34]. Table 2 shows the crushing performance for all types of specimens under quasi-static axial crushing test. It was shown that specimen A3L has the highest energy absorption and specific energy absorption, which were 63.82 J and 3.69 J/g. This value is an increase of nearly 230% of EA value and 125% of SEA value from specimen A1S, which has the lowest value of EA and SEA among the specimens. From the data recorded, specimen S4S has the highest CFE value among the specimens, 0.56. In order to enhance comprehension, ANOVA was employed to determine the impact of reinforcement domination, mesh size, stacking structure of reinforcements, and their interactions on the energy absorption performance of BFAMRP composites. Table 3 presents the ANOVA findings regarding the energy absorption performance of BFAMRP composites during a quasi-static crushing test.

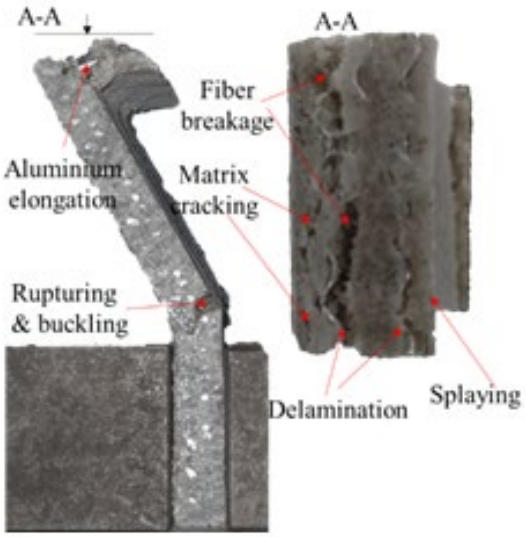

Fig. 7 *Failure morphologies of A3L specimens under quasi-static axial crushing test*

Table 2 *Energy absorption performance of BFAMRP composites under Quasi-static axial crushing test*

Specimens	EA (J)	F_{max} (kN)	F_{avg} (kN)	SEA (J/g)	CFE
A1S	19.37	5.31	2.65	1.64	0.50
	(2.33)	(0.54)	(0.35)	(0.11)	(0.07)
A1L	27.29	6.24	2.70	2.12	0.54
	(5.61)	(1.03)	(0.50)	(0.28)	(0.03)
S2S	27.71	4.64	2.49	2.24	0.44
	(1.31)	(0.14)	(0.06)	(0.14)	(0.06)
S2L	40.45	7.67	3.80	2.79	0.50
	(3.41)	(0.22)	(0.44)	(0.21)	(0.07)
A3S	54.20	8.92	3.43	3.22	0.45
	(3.47)	(0.29)	(0.80)	(0.12)	(0.03)
A3L	63.82	10.24	4.70	3.69	0.51
	(8.38)	(0.53)	(0.12)	(0.31)	(0.09)
S4S	31.28	7.59	3.71	2.45	0.56
	(2.85)	(0.48)	(0.31)	(0.13)	(0.11)
S4L	45.04	8.21	4.13	2.74	0.50
	(2.33)	(0.45)	(0.35)	(0.12)	(0.02)

Table 3 *ANOVA result of energy absorption performance of BFAMRP composites under quasi-static axial crushing test*

Source	Df	P-value	Significant
a) EA (J)			
Reinforcement Domination (RD)	1	**0.000**	***
Mesh Size (MS)	1	**0.000**	***
Stacking structure (SS)	1	**0.008**	**
RD * MS	1	0.694	ns
RD * SS	1	**0.000**	***
MS * SS	1	0.204	ns
Error	17		
Total	23		
b) SEA (J/g)			
Reinforcement Domination (RD)	1	**0.000**	***
Mesh Size (MS)	1	**0.000**	***
Stacking structure (SS)	1	0.150	ns
RD * MS	1	0.357	ns
RD * SS	1	**0.000**	***
MS * SS	1	0.719	ns
Error	17		
Total	23		
c) CFE			
Reinforcement Domination (RD)	1	0.600	ns
Mesh Size (MS)	1	0.385	ns
Stacking structure (SS)	1	1.000	ns
RD * MS	1	0.417	ns
RD * SS	1	0.083	ns
MS * SS	1	0.385	ns
Error	17		
Total	23		

*** Significantly different at p<0.001
** Significantly different at p<0.01
* Significantly different at p<0.05
ns Not Significant

The analysis of the associated P-values revealed a substantial impact of the reinforcement dominating factor on the EA and SEA of the specimens during the quasi-static crushing test. The mesh size factor has comparable effects to the dominance of reinforcement, greatly impacting almost all crushing properties except for CFE. The stacking structure had a substantial impact on EA. Conversely, a high P-value indicates that the factors have a

Int. Journal of Integrated Engineering Vol. 16 No. 6 (2024) p. 130-144

negligible impact on CFE. Figure 8 illustrates the primary impact graphs showcasing the energy absorption performance of BFAMRP composites.

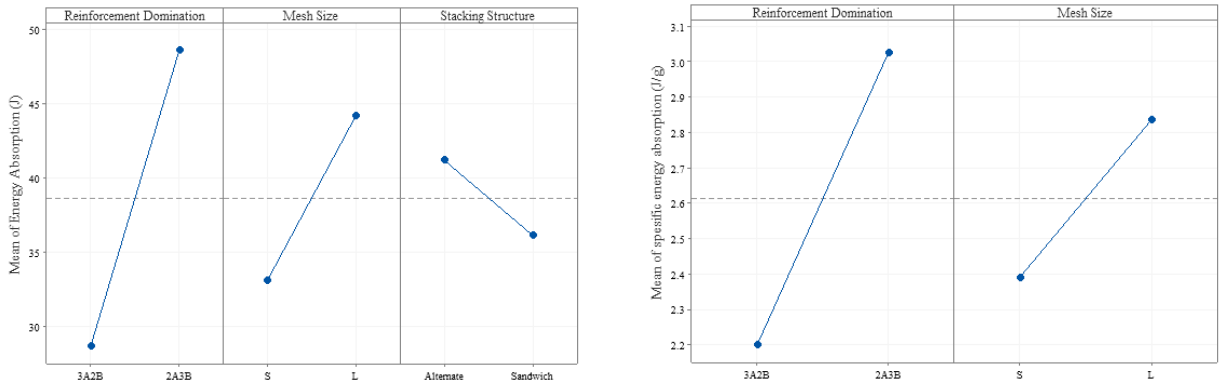

Fig. 8 *Main effect plots of (a) EA; and (b) SEA of BFAMRP composites under quasi-static axial crushing test*

It was observed from Figure 8 that composites dominated by 2A3B reinforcement tended to have greater energy absorption, *F*max, *F*avg, and SEA than composites dominated by 3A2B reinforcement. This outcome was anticipated, given that fibre has a propensity to absorb more energy than metal via the formation and propagation of fractures and fissures [34]. The composite material consisting of 3B2A demonstrated a notably elevated EA value, consequently affecting the SEA value in a significant way. The incorporation of bamboo fibres, which are lighter in weight compared to the aluminium mesh, led to a higher SEA value for this particular specimen. This discovery sets it apart from the sample, which consists of three metal components and two bamboo fibre components.

The examination of the main effect plots unveiled a distinct association between the mesh size and the energy absorption performance, particularly in relation to EA and SEA. Specimens comprising a larger mesh size demonstrated enhanced energy absorption capabilities in comparison to specimens featuring a smaller mesh size. The EA values exhibited a substantial surge of 46%. Furthermore, the SEA values demonstrated a moderate growth of 29%. The results validated the importance of mesh size in reinforcing composites for applications involving energy absorption structures.

In relation to the stacking structure factor, the main effect plots demonstrated that its impact on EA values was statistically significant. The sandwich structure demonstrated fewer outstanding values in comparison to the alternative type structure. When contrasting specimens, A3L (alternate structure) with B/A/B/A/B demonstrated superior EA values of 63.82 J respectively, over specimen S4L (sandwich structure) with A/B/B/B/A (45.04J for EA). The energy absorption performance may have been impacted by the positioning of an aluminium mesh sheet within the bamboo fibre layer, given that the ductility of aluminium counterbalanced the brittleness of the fibres during crushing failure. As a consequence, the load-displacement curve became considerably more consistent, leading to a substantial increase in the EA values of the specific specimen in question.

3.2 Dynamic Impact Test

In order to enable comparison, the load-displacement curve obtained from the quasi-static crushing test was aligned with that of the dynamic impact test. Figure 9 presents a comparison between the load-displacement curves of specimen A3L in quasi-static crushing and dynamic impact testing. The figure illustrates that the dynamic impact test resulted in a significantly higher maximum load than the quasi-static crushing test. Nevertheless, the displacement of specimens during the dynamic impact test exhibited a reduced magnitude of displacement, leading to failure compared to specimens subjected to the quasi-static crushing test. This suggests that the specimen is capable of absorbing kinetic energy during the impact process [35]. Delamination extends extensively into the composite material of specimens subjected to high compression rates, leading to a stress-displacement response characterised by low frequency and deeply serrated patterns [36].

Figure 10 displays A3L composite specimens that experienced failure during the dynamic impact test. When comparing the specimens that failed in the quasi-static crushing test (Figure 7) to the dynamic-impact specimens, there were small variations in the way they were crushed. Specimens exhibited larger splaying zones and matrix cracking. The presence of severe delamination was clearly evident. The interaction between the brittle bamboo fibre layer and the plastic aluminium sheet had a notable effect on the axial splaying behaviour.

The various types of crushing in dynamic impact can be categorised as matrix cracking, fibre breaking, splaying, and delamination. In general, dynamic impact resulted in more damage morphologies compared to quasi-static crushing. One notable discovery from this investigation was the absence of catastrophic failure in terms of smaller shards of composites, which is a regular occurrence in FRP composite materials. The aluminium mesh sheet enhances the structural integrity of the composite construction, even in cases of severe damage, by maintaining a certain level of strength and preventing catastrophic collapse [37].

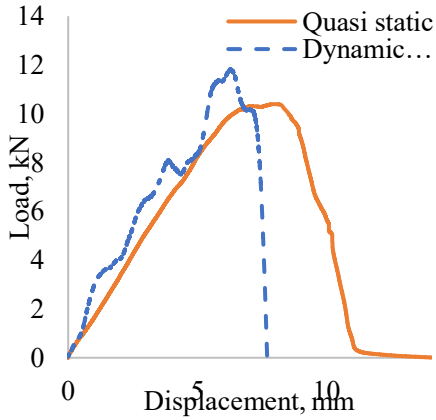

Fig. 9 *Comparative load-displacement curves of A3L specimen under quasi-static axial crushing and dynamic impact loads*

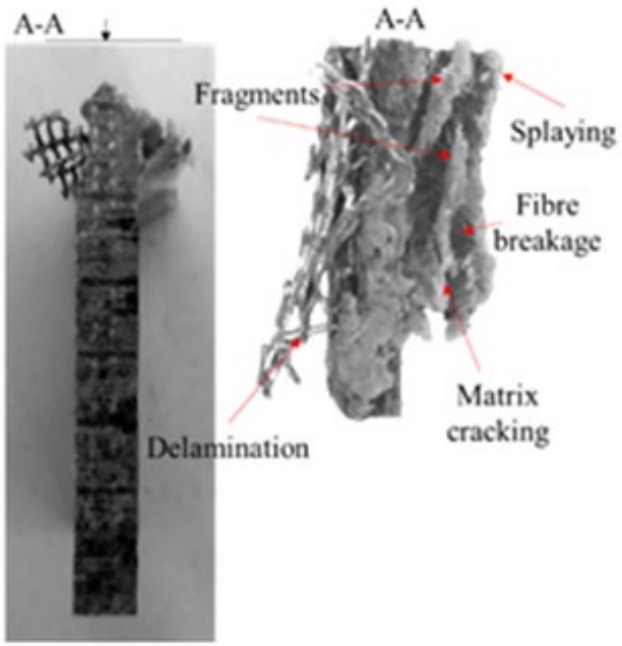

Fig. 10 *Failure morphologies of A3L specimen under dynamic impact loads*

Table 4 shows the crushing performance for all types of specimens under dynamic impact test. It was shown that specimen A3L has the highest energy absorption and specific energy absorption, which were 57.57 J and 3.25 J/g. This value is an increase of nearly 273% of EA value and 148% of SEA value from specimen A1S, which has the lowest value of EA and SEA among the specimens. From the data recorded, specimen A3L also has the highest CFE value among the specimens with 0.63. Table 5 presents the ANOVA findings for the energy absorption performance of BFAMRP composites during a dynamic impact test. According to the P-values, the reinforcing dominating factor had a notable impact on the energy absorption performances of the specimens during the dynamic impact test. Furthermore, the statistical analysis revealed that the mesh size factor had a substantial impact on both SEA and CFE values. The stacking structure has a substantial impact on the EA and SEA values.

Int. Journal of Integrated Engineering Vol. 16 No. 6 (2024) p. 130-144

Table 4 *Energy absorption performance of BFAMRP composites under dynamic impact test*

Specimens	EA J	F_{max} kN	F_{avg} kN	SEA J/g	CFE
A1S	15.42	6.99	3.67	1.31	0.52
	(0.44)	(0.12)	(0.20)	(0.05)	(0.02)
A1L	27.15	6.78	3.71	2.17	0.55
	(2.01)	(0.49)	(0.24)	(0.21)	(0.07)
S2S	26.51	7.34	3.65	2.01	0.50
	(6.54)	(1.56)	(0.83)	(0.32)	(0.01)
S2L	32.83	9.86	4.38	2.54	0.44
	(5.02)	(1.30)	(0.49)	(0.56)	(0.01)
A3S	48.43	11.09	5.92	2.87	0.54
	(3.62)	(0.81)	(0.27)	(0.21)	(0.03)
A3L	57.57	12.26	7.69	3.25	0.63
	(3.06)	(1.21)	(0.17)	(0.49)	(0.05)
S4S	22.14	9.07	5.18	1.72	0.58
	(2.10)	(1.49)	(0.50)	(0.15)	(0.05)
S4L	30.69	9.03	5.02	2.35	0.55
	(5.46)	(1.13)	(0.89)	(0.33)	(0.04)

Table 5 *ANOVA result of energy absorption performance of BFAMRP composites under dynamic impact test*

Source	Df	P-value	Significant
a) EA (J)			
Reinforcement Domination (RD)	1	**0.000**	***
Mesh Size (MS)	1	0.114	ns
Stacking structure (SS)	1	**0.000**	***
RD * MS	1	0.094	ns
RD * SS	1	**0.000**	***
MS * SS	1	0.931	ns
Error	17		
Total	23		
b) SEA (J/g)			
Reinforcement Domination (RD)	1	**0.009**	**
Mesh Size (MS)	1	**0.038**	*
Stacking structure (SS)	1	**0.031**	*
RD * MS	1	0.139	ns
RD * SS	1	**0.004**	**
MS * SS	1	0.942	ns
Error	17		
Total	23		
c) CFE			
Reinforcement Domination (RD)	1	**0.001**	***
Mesh Size (MS)	1	**0.043**	*
Stacking structure (SS)	1	0.518	ns
RD * MS	1	0.222	ns
RD * SS	1	0.112	ns
MS * SS	1	**0.007**	**
Error	17		
Total	23		

*** Significantly different at p<0.001
** Significantly different at p<0.01
* Significantly different at p<0.05
ns Not Significant

Figure 11 exhibits the primary effect plots of all factors that have a substantial impact on the energy absorption performance. The findings demonstrated that the CFE value derived from the dynamic impact test was notably influenced by the dominance of reinforcement and the size of the mesh, unlike the CFE value obtained from the quasi-static test, which showed no impact from these factors. The figure illustrates the primary impact plots of three parameters that significantly influence the energy absorption performance

obtained in the dynamic impact test. Specimens with a dominant 2A3B reinforcement showed significantly greater levels of energy absorption performance compared to composites with a dominant 3A2B reinforcement. Similar results were noted while analysing the energy absorption performance in quasi-static crushing experiments.

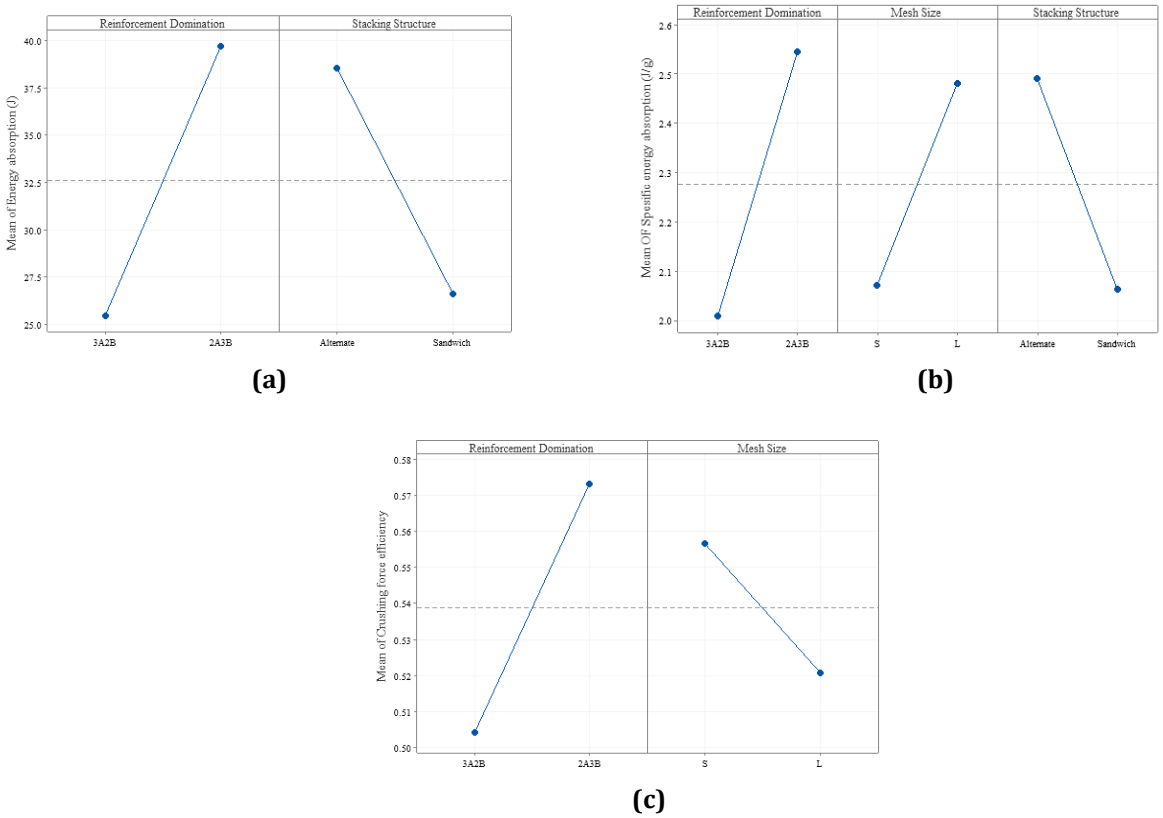

Fig. 11 *Main effect plots of (a)EA; (b)SEA; and (c)CFE of BFAMRP composites under dynamic impact test*

The energy absorption performance, specifically the SEA and CFE values, were considerably influenced by the mesh size of the aluminium expanded mesh sheet. The testing results showed that specimens with a smaller mesh size of aluminium mesh sheet had a lower SEA value compared to specimens with a larger mesh size. The performance of the CFE index showed a contrasting condition compared to the SEA plot. The results of this study offered empirical proof that mesh size plays a crucial role in strengthening composites for applications involving energy absorption structures.

Regarding the stacking structure factor, the examination of the main effect plot revealed a statistically significant impact on almost all energy absorption performances, with the exception of CFE. Researchers frequently prefer sandwich designs for applications involving long-term energy absorption in structures. The absence of interaction between the reinforcement material and matrix in the sandwich construction exhibited the capacity to efficiently alleviate and forestall different delamination or interlaminar fracture problems that may occur during the crushing process. However, this study reveals a contrasting scenario where the alternative structural structure exhibited greater levels of SEA and CFE values than the sandwich structural arrangement. The improved cohesiveness of this composite material can be attributed to the treatment process of the bamboo fibres. This treatment enhances the formation of a more robust connection between the bamboo fibres and the matrix components [38], [39]. In addition, the use of aluminium mesh sheets, rather than traditional aluminium sheets, enhances the bond between the metal sheet and matrix [27]. The described strategy, when applied alongside the vacuum infusion process, helps to reduce the incidence of void-related difficulties that are typically found in composite specimens due to production processes like vacuum bagging or hand lay-up process [40].

4. Conclusion

In this experiment, eight types of BFAMRP composite were fabricated and tested under quasi-static axial crushing and dynamic impact tests. The energy absorption performance and failure morphology were analyzed from both tests, followed by an ANOVA analysis of the results.

Specimen A3L exhibited superior energy absorption performance compared to all other specimens in both quasi-static crushing and dynamic impact tests. The crushing mechanism in all specimens showed a combination of gradual failure and buckling behaviour, with the chamfer acting as a trigger mechanism to generate a more efficient failure mode, facilitating the absorption of a significantly larger amount of energy during crushing.

The composite material containing mostly bamboo fibres (2A3B) outperformed the one with mostly aluminium mesh (3A2B) in terms of absorbed energy (EA) by up to 75%, specific energy absorption (SEA) by up to 28%, and crush force efficiency (CFE) by up to 14.5% during the dynamic impact test. The quasi-static test yielded smaller results for both EA and SEA compared to the dynamic impact test, with an empirical increase of 58% for EA and 33% for SEA noted. CFE values during the quasi-static crushing test were approximately 10% lower than those from the dynamic impact test, suggesting that the innovative composites demonstrated improved stability and effectively regulated the crushing process, as expected in real crash scenarios.

ANOVA results indicated that both reinforcement domination and mesh size significantly impacted crushing performance, except for the CFE value in the quasi-static crushing test. The variance in dynamic impact test results differed from the crushing performance, with reinforcement domination and stacking structure being the prominent factors influencing performance. Additionally, the CFE value was greatly affected by the dominance of reinforcement and mesh size.

Acknowledgements

Communication of this research is made possible through monetary assistance by Universiti Tun Hussein Onn Malaysia and the UTHM Publisher's Office via Publication Fund E15216. In addition, the authors thank the Bamboo Research Centre (BambooRC), Faculty of Engineering Technology, Faculty of Mechanical and Manufacturing Engineering, Universiti Tun Hussein Onn Malaysia and Advanced Technology Centre (ADTEC) Batu Pahat for their support in this research.

Conflict of Interest

The authors declare that there is no conflict of interest regarding the publication of the paper.

Author Contribution

The authors confirm their contribution to the paper as follows: ***study conception and design:*** *Nik Ainun Nik Ismail, Mohd Nazrul Roslan;* ***data collection:*** *Nik Ainun Nik Ismail;* ***analysis and interpretation of results:*** *Nik Ainun Nik Ismail, Mohd Nazrul Roslan, Al Emran Ismail, Mohd Khairun Anwar Uyup;* ***draft manuscript preparation:*** *Nik Ainun Nik Ismail, Mohd Nazrul Roslan. All authors reviewed the results and approved the final version of the manuscript.*

References

[1] Lu, G., & Yu, T. (2003). Energy Absorption of Structures and Materials. In CRC Press , Woodhead Publishing Limited (1st Editio). CRC Press and Woodhead Publishing Limited. https://doi.org/10.1201/9780203484128

[2] Baroutaji, A., Sajjia, M., & Olabi, A. (2017). Thin-Walled Structures On the crashworthiness performance of thin-walled energy absorbers : Recent advances and future developments. Thin Walled Structures, 118(May), 137–163. https://doi.org/10.1016/j.tws.2017.05.018

[3] Liu, X., Belkassem, B., Jonet, A., Lecompte, D., Van Hemelrijck, D., Pintelon, R., & Pyl, L. (2019). Experimental investigation of energy absorptio n behaviour of circular carbon/epoxy composite tubes under quasi-static and dynamic crush loading. Composite Structures, 227(June), 111266. https://doi.org/10.1016/j.compstruct.2019.111266

[4] Boria, S., Obradovic, J., & Belingardi, G. (2015). Experimental and numerical investigations of the impact behaviour of composite frontal crash structures. Composites Part B: Engineering, 79, 20–27. https://doi.org/10.1016/j.compositesb.2015.04.016

[5] Riccio, A., Raimondo, A., Di Caprio, F., Fusco, M., & Sanità, P. (2018). Experimental and numerical investigation on the crashworthiness of a composite fuselage sub-floor support system. Composites Part B: Engineering, 150(April), 93–103. https://doi.org/10.1016/j.compositesb.2018.05.044

[6] Zhang, Z., Liu, S., & Tang, Z. (2011). Comparisons of honeycomb sandwich and foam-filled cylindrical columns under axial crushing loads. Thin-Walled Structures, 49(9), 1071–1079. https://doi.org/10.1016/j.tws.2011.03.017

[7] Niknejad, A., Assaee, H., Elahi, S. A., & Golriz, A. (2013). Flattening process of empty and polyurethane foam-filled E-glass/vinylester composite tubes - An experimental study. Composite Structures, 100, 479–492. https://doi.org/10.1016/j.compstruct.2013.01.009

[8] Sivakumar, D., Ng, L. F., Ng, J. W., & Selamat, M. Z. (2017). Failure Analysis of Hybrid Fibre Reinforced Plastics for Bolted Joint under Thermal Effect. Journal of Mechanical Engineering, 1(1), 141–156.
[9] Nurul Fazita, M. R., Abdul Khalil, H. P. S., Nor Amira Izzati, A., & Rizal, S. (2018). Effects of strain rate on failure mechanisms and energy absorption in polymer composites. In Failure Analysis in Biocomposites, Fibre-Reinforced Composites and Hybrid Composites (pp. 51–78). Elsevier Ltd. https://doi.org/10.1016/B978-0-08-102293-1.00003-6
[10] Okubo, K., Fujii, T., & Yamamoto, Y. (2004). Development of bamboo-based polymer composites and their mechanical properties. Composites Part A: Applied Science and Manufacturing, 35(3), 377–383. https://doi.org/10.1016/j.compositesa.2003.09.017
[11] Sen, T., & Reddy, H. N. J. (2011). Application of Sisal , Bamboo , Coir and Jute Natural Composites in Structural Upgradation. International Journal of Innovation, Maagement and Technology, 2(3), 186–191.
[12] Rassiah, K., & Megat Ahmad, M. M. H. (2013). A Review On Mechanical Properties Of Bamboo Fiber Reinforced Polymer Composite. Australian Journal of Basic and Applied Sciences, 7(8), 247–253.
[13] Mohanty, A. K., Misra, M., & Hinrichsen, G. (2000). Biofibres, biodegradable polymers and biocomposites: An overview. Macromolecular Materials and Engineering, 276–277, 1–24. https://doi.org/10.1002/(SICI)1439-2054(20000301)276
[14] Supian, A. B. M., Sapuan, S. M., Zuhri, M. Y. M., Zainudin, E. S., & Ya, H. H. (2018). Hybrid reinforced thermoset polymer composite in energy absorption tube application: A review. Defence Technology, 14(4), 291–305. https://doi.org/10.1016/j.dt.2018.04.004
[15] Shewale, J., Choudhari, C., & Bankoti, A. (2022). Carbon and natural fiber reinforced polymer hybrid composite: Processes, applications, and challenges. Journal of Mechanical Engineering and Sciences (JMES), 16(2), 8873–8891. https://doi.org/10.15282/jmes.16.2.2022.06.0702
[16] Siva Sai Sundar Singh, S., & Madhu, S. (2022). Enhancement of tensile strength of bamboo fibre reinforced titanium laminate by addition of portunus filler compared with bamboo titanium composite. Materials Today: Proceedings, 79, 127–131. https://doi.org/10.1016/j.matpr.2022.10.084
[17] Prabhakar, C. G., Anand Babu, K., Kataraki, P. S., & Reddy, S. (2022). A review on natural fibers and mechanical properties of banyan and banana fibers composites. Materials Today: Proceedings, 54, 348–358. https://doi.org/10.1016/j.matpr.2021.09.300
[18] Muthukannan, M., Shankar Kannan, P., Selwin, M., & Kathiravan, T. (2023). Experimental investigation of mechanical properties of Palm - Bamboo – Glass fibre composites. Materials Today: Proceedings, xxxx. https://doi.org/10.1016/j.matpr.2023.01.377
[19] Chandramohan, D., Dhanashekar, M., Sathish, T., & Kumar, S. D. (2021). Materials Today : Proceedings Characterisation of hybrid Aloe Vera / Bamboo / Palm / Kevlar fibers for better mechanical properties. Materials Today: Proceedings, 37, 2223–2227. https://doi.org/10.1016/j.matpr.2020.07.657
[20] Haldar, P., Modak, N., & Sutradhar, G. (2017). Comparative Evaluation of Mechanical Properties of Sisal-Epoxy Composites with and Without Addition of Aluminium Powder. Materials Today: Proceedings, 4(2), 3397–3406. https://doi.org/10.1016/j.matpr.2017.02.228
[21] Subash, S., Jones, B. S., Happy, J. J., Raja, J. E., Savio, K. A., & Ganesh, M. (2022). Materials Today : Proceedings Preparation and characterisation of Silk / Bamboo / Glass nano polymer composites. Materials Today: Proceedings, 64, 298–301. https://doi.org/10.1016/j.matpr.2022.04.570
[22] Ramasamy, M., Arul Daniel, A., Nithya, M., Sathees Kumar, S., & Pugazhenthi, R. (2020). Characterisation of natural – Synthetic fiber reinforced epoxy based composite – Hybridisation of kenaf fiber and kevlar fiber. Materials Today: Proceedings. https://doi.org/10.1016/j.matpr.2020.07.243
[23] Zhu, G., Sun, G., Liu, Q., Li, G., & Li, Q. (2017). On crushing characteristics of different configurations of metal-composites hybrid tubes. Composite Structures, 175, 58–69. https://doi.org/10.1016/j.compstruct.2017.04.072
[24] Lebaupin, Y., Friedli, J., Caglar, B., Piccand, M., Pasquier, R., & Michaud, V. (2019). Crushing and intrusion resistance improvement of aluminum beams by carbon/epoxy composite patches. Composite Structures, 226(April), 111235. https://doi.org/10.1016/j.compstruct.2019.111235
[25] Gonzalez-Canche, N. G., Flores-Johnson, E. A., & Carrillo, J. G. (2017). Mechanical characterisation of fiber metal laminate based on aramid fiber reinforced polypropylene. Composite Structures, 172, 259–266. https://doi.org/10.1016/j.compstruct.2017.02.100
[26] Megeri, S., & Naik, G. N. (2021). Numerical studies of the low velocity impact behaviour on hybrid fiber metal laminates. Materials Today: Proceedings, 44, 1860–1864. https://doi.org/10.1016/j.matpr.2020.12.030
[27] Megahed, A. A., Abd El-Wadoud, F., Wagih, A., & Kabeel, A. M. (2021). Effect of incorporating aluminum wire mesh on the notched and un-notched strengths of glass fiber/epoxy composites. Composite Structures, 263(February), 113695. https://doi.org/10.1016/j.compstruct.2021.113695

[28] Arun Prakash, V. R., & Julyes Jaisingh, S. (2018). Mechanical strength behaviour of silane treated E-glass fibre, Al-6061 and SS-304 wire mesh reinforced epoxy resin Hybrid composites. Defence Technology. https://doi.org/10.1016/j.dt.2018.01.006
[29] Chen, Y., Ye, L., Fu, K., & Han, X. (2018). Transition from buckling to progressive failure during quasi-static in-plane crushing of CF/EP composite sandwich panels. Composites Science and Technology, 168(May), 133–144. https://doi:10.1016/j.compscitech.2018.09.017
[30] Chen, Y., Cheng, X., Fu, K., & Ye, L. (2020). Failure characteristics and multi-objective optimisation of CF/EP composite sandwich panels under edgewise crushing. International Journal of Mechanical Sciences, 183(March). https://doi.org/10.1016/j.ijmecsci.2020.105829
[31] Liu, H., Falzon, B. G., & Dear, J. P. (2019). An experimental and numerical study on the crush behaviour of hybrid unidirectional/woven carbon-fibre reinforced composite laminates. International Journal of Mechanical Sciences, 164(September). https://doi.org/10.1016/j.ijmecsci.2019.105160
[32] Chen, Y., Ye, L., Fu, K., & Han, X. (2018). Transition from buckling to progressive failure during quasi-static in-plane crushing of CF/EP composite sandwich panels. Composites Science and Technology, 168(May), 133–144. https://doi.org/10.1016/j.compscitech.2018.09.017
[33] Aodkeng, S., Sinthupinyo, S., Chamnankid, B., Hanpongpun, W., & Chaipanich, A. (2022). Effect of carbon nanotubes/clay hybrid composite on mechanical properties, hydration heat and thermal analysis of cement-based materials. Construction and Building Materials, 320(December 2021), 126212. https://doi.org/10.1016/j.conbuildmat.2021.126212
[34] Yang, H., Lei, H., Lu, G., Zhang, Z., Li, X., & Liu, Y. (2020). Energy absorption and failure pattern of hybrid composite tubes under quasi-static axial compression. Composites Part B, 198(May), 108–217. https://doi.org/10.1016/j.compositesb.2020.108217
[35] Roslan, M. N. (2018). Energy absorption performance of braided basalt reinforced composite tubes under axial loads (Issue June). Universiti Teknologi Malaysia.
[36] Lavoie, J. A., & Kellas, S. (1996). Dynamic crush tests of energy-absorbing laminated composite plates. Composites Part A: Applied Science and Manufacturing, 27(6), 467–475. https://doi.org/10.1016/1359835X(95)00058-A
[37] Mansor, M. A., Ahmad, Z., & Abdullah, M. R. (2022). Crashworthiness capability of thin-walled fibre metal laminate tubes under axial crushing. Engineering Structures, 252(November 2021), 113660. https://doi.org/10.1016/j.engstruct.2021.113660
[38] Huang, J.-K., & Young, W.-B. (2019). The mechanical, hygral, and interfacial strength of continuous bamboo fiber reinforced epoxy composites. Composites: Part B, 166, 272–283. https://doi.org/10.1016/j.compositesb.2018.12.013
[39] Sánchez, M. L., Patiño, W., & Cárdenas, J. (2020). Physical-mechanical properties of bamboo fibers-reinforced biocomposites: Influence of surface treatment of fibers. Journal of Building Engineering, 28(May 2019). https://doi.org/10.1016/j.jobe.2019.101058
[40] Abdurohman, K., Satrio, T., Muzayadah, N. L., & Teten. (2018). A comparison process between hand lay-up, vacuum infusion and vacuum bagging method toward e-glass EW 185/lycal composites. Journal of Physics: Conference Series, 1130(1). https://doi.org/10.1088/1742-6596/1130/1/012018